Moiré Is Different

Wenyuan Shi[1]

[1] Western Reserve Academy, Ohio, United States

Correspondence: Wenyuan Shi, Western Reserve Academy, Ohio, United States. E-mail: alex.shiwenyuan@gmail.com

Abstract

Graphene, as the thinnest material ever found, exhibits unconventionally relativistic behaviour of Dirac fermions. However, unusual phenomena (such as superconductivity) arise when stacking two graphene layers and twisting the bilayer graphene. The relativistic Dirac fermion in graphene has been widely studied and understood, but the large change observed in twisted bilayer graphene (TBG) is intriguing and still unclear because only van der Waals force (vdW) interlayer interaction is added from graphene to TBG and such a very weak interaction is expected to play a negligible role. To understand such dramatic variation, we studied the electronic structures of monolayer, bilayer and twisted bilayer graphene. Twisted bilayer graphene creates different moiré patterns when turned at different angles. We proposed tight-binding and effective continuum models and thereby drafted a computer code to calculate their electronic structures. Our calculated results show that the electronic structure of twisted bilayer graphene changes significantly even by a tiny twist. When bilayer graphene is twisted at special "magic angles", flat bands appear. We examined how these flat bands are created, their properties and the relevance to some unconventional physical property such as superconductivity. We conclude that in the nanoscopic scale, similar looking atomic structures can create vastly different electronic structures. Like how P. W. Anderson stated that similar looking fields in science can have differences in his article "More is Different", similar moiré patterns in twisted bilayer graphene can produce different electronic structures.

Keywords: Twisted Bilayer Graphene, Electron Band Structure, Density of States, Magic Angle

1. Introduction

In 1972, physicist Phillip W. Anderson wrote an article called "More is Different". In the article (Anderson, 1972), he explained how although symmetry is of great importance to physics, objects that appear symmetric may not be actually symmetric at the quantum scale. The physical laws that govern an object may also be un-symmetric. Through this, he emphasized how scientists' focus on reductionism may limit scientific advancement. He also expressed that the common view of science having a hierarchy (biology is applied chemistry, physics is applied math, etc.) is wrong. Things that seems similar at first look may have large deviations. At the quantum level, even tiny changes could create huge differences.

One material where a tiny change can create a huge difference is twisted bilayer graphene (TBG). As the thinnest known material, graphene has been found to exhibit unconventional behaviour of relativistic Dirac fermions, for example, a linear dispersive band in the vicinity of the zone corner of its reciprocal Brillouin zone. Bilayer graphene is when two layers of graphene are laid on top of each other. By putting a twist between the two layers, special "moiré patterns" can be created. A tiny change in angle could create a vastly different moiré pattern. However, some fascinating phenomena such as superconductivity and other novel strong-correlation properties(Bistritzer & MacDonald, 2011; Cao, Fatemi, Demir, Fang, Tomarken, Luo, Sanchez-Yamagishi, Watanabe, Taniguchi, Kaxiras, Ashoori, & Jarillo-Herrero, 2018; Cao, Fatemi, Fang, Watanabe, Taniguchi, Kaxiras, & Jarillo-Herrero, 2018), which are unconceivable in graphene, are found to arise in TBG. Such a big change observed from graphene to TBG is very intriguing but unclear, because it is very counterintuitive to ascribe such a big change to the tiny change in twist or to the very weak van der Waals force (vdW) interlayer interaction.To comprehend the huge difference due to tiny change in TBG, we examined the electronic properties of graphene and conventional bilayer graphene, then created twisted bilayer graphene and finally investigated the electronic band structure of TBG within tight binding approximation and effective continuum model. At some specific angles, dubbed "magic angles" in a moiré superlattice, a special "flat band" shows up merely due to the weak vdW interlayer interaction. We also examined how the model of TBG changes at and around magic angles

through the electronic density of states. The electrons move extremely slowly in the flat band near the Fermi level, increasing the Coulomb interaction between each other, or the so-called strong correlation effect, which can help us understand the emergence of superconductivity relevant to high-Tc superconductors(Cao, Fatemi, Demir, Fang, Tomarken, Luo, Sanchez-Yamagishi, Watanabe, Taniguchi, Kaxiras, Ashoori, & Jarillo-Herrero, 2018; Cao, Fatemi, Fang, Watanabe, Taniguchi, Kaxiras, & Jarillo-Herrero, 2018).

2. Model, Results, and Discussions

2.1 Atomic and Electronic Structure of Monolayer Graphene

We will start from graphite; graphite is everywhere in our daily life, for example, in the pencils we use. It is an anisotropic structure with many single-atomic layers stacking together. More than ten years ago, two physicists Dr. Andre Geim and Dr. Konstantin Novoselov from University of Manchester succeeded in obtaining one such atomic-thick layer (dubbed graphene) by mechanically exfoliating graphite using Scotch tape. They were awarded the Nobel Prize for significant contributions(Novoselov, Geim, Morozov, Jiang, Zhang, Dubonos, Grigorieva, & Firsov, 2004; Novoselov, Geim, Morozov, Jiang, & Katsnelson, 2005) in Physics in 2010. As shown in Figure 1, graphene is a hexagonal lattice pattern of a carbon atomic layer. Graphene is the thinnest material ever found and has many novel properties: it is strong, light, and a good conductor of electricity.
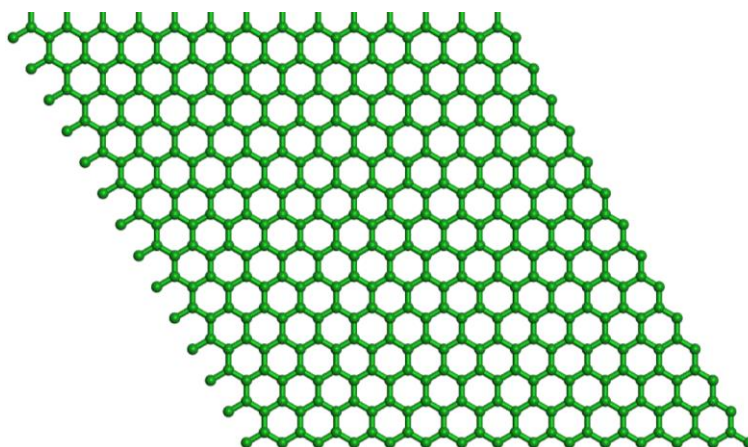

Figure 1. Single-atomic-thick structure of graphene

The simplest unit or the primitive structure of graphene has atom A and B, as seen from Figure 2 (Left). Defining the distance between atom A and B as a, we can write the unit-cell lattice vectors as $\vec{a}_1 = a_0 (-\frac{\sqrt{3}}{2}, \frac{1}{2}, 0), \vec{a}_2 = a_0 (0,1,0)$, $\vec{a}_3 = c_0 (0, 0, 1)$, where $a_0 = \sqrt{3}a$. To study the electronic structure, it will be more convenient to work in the reciprocal k space. To calculate the unit vectors $(\vec{b}_1, \vec{b}_2, \vec{b}_3)$ in reciprocal space, using the following formulae:

$$\mathbf{b}_1 = 2\pi \frac{\mathbf{a}_2 \times \mathbf{a}_3}{\mathbf{a}_1 \cdot (\mathbf{a}_2 \times \mathbf{a}_3)}$$
$$\mathbf{b}_2 = 2\pi \frac{\mathbf{a}_3 \times \mathbf{a}_1}{\mathbf{a}_2 \cdot (\mathbf{a}_3 \times \mathbf{a}_1)}$$
$$\mathbf{b}_3 = 2\pi \frac{\mathbf{a}_1 \times \mathbf{a}_2}{\mathbf{a}_3 \cdot (\mathbf{a}_1 \times \mathbf{a}_2)}$$

(1)

we have $\vec{b}_1 = \frac{4\pi}{\sqrt{3}a_0} (1, 0, 0)$ and $\vec{b}_2 = \frac{4\pi}{\sqrt{3}a_0} (\frac{1}{2}, \frac{\sqrt{3}}{2}, 0)$, as given in Figure 2 (Right).
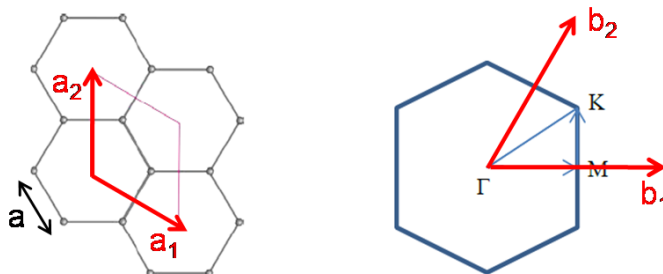
Figure 2. (Left) The unit-cell lattice vectors of graphene. (Right) The reciprocal unit vectors of graphene

Electron motion in graphene is governed by the Schrödinger equation H $\Phi(x) = \varepsilon\Phi(x)$, in which $\Phi(x)$ is wave function of the system, H is the system Hamiltonian, and ε is the eigenvalue of the wave function. The π-electronic wave function $\Phi(x)$ of graphene can be constructed by combing the p_z orbitals on both A and B sites in the Bloch type(Wallace, 1947; Moon & Koshino, 2013; Koshino, 2015):

$$\Phi(x) = \Sigma_{RA,\,RB}\,[e^{i(k \cdot R_A)}\,A\,\phi_A(x - R_A) + e^{i(k \cdot R_B)}\,B\,\phi_B(x - R_B)] \tag{2}$$

Where R_A and R_B are the translational lattice vectors and k is the wave vector in reciprocal space. By multiplying $\phi^*_A(0)$ to the Schrödinger equation H $\Phi(x) = \varepsilon\Phi(x)$ and integrating it in the whole real space —$\int d\tau \phi^*_A(0)$H $\Phi(x)$ = $\int d\tau \phi^*_A(0)\varepsilon\Phi(x)$ — we will obtain the following equations:

$$(\varepsilon_A - \varepsilon)A + E_1[e^{-ik_x a} + 2e^{\frac{ik_x a}{2}}\cos\left(\frac{\sqrt{3}k_y a}{2}\right)]\,B\ = 0 \tag{3}$$

$$E_1[e^{ik_x a} + 2e^{-\frac{ik_x a}{2}}\cos\left(\frac{\sqrt{3}k_y a}{2}\right)]\ + (\varepsilon_B - \varepsilon)\,B = 0 \tag{4}$$

which can be described using the following matrix:

$$\begin{bmatrix} \varepsilon_A - \varepsilon & E_1[e^{-ik_x a} + 2e^{\frac{ik_x a}{2}}\cos\left(\frac{\sqrt{3}k_y a}{2}\right)] \\ E_1[e^{ik_x a} + 2e^{-\frac{ik_x a}{2}}\cos\left(\frac{\sqrt{3}k_y a}{2}\right)] & \varepsilon_B - \varepsilon \end{bmatrix}\begin{bmatrix} A \\ B \end{bmatrix} = 0 \tag{5}$$

where ε_A (or ε_B, is the on-site energy and here for simplicity we set $\varepsilon_B = \varepsilon_A = 0$) refers to the eigenvalue of the π-electronic in the carbon atom and $E_1 = \int d\tau \phi^*_A H \phi_B$ is defined as the electronic hopping energy between the nearest A and B atoms. From here, we can obtain the following formula of the dispersive electronic band structure, which is plotted in Figure 3.

$$E^{(\pm)}(k) = \pm\gamma\sqrt{1 + 4\cos\left(\frac{\sqrt{3}k_x a_0}{2}\right)\cos\left(\frac{k_y a_0}{2}\right) + 4\cos^2\left(\frac{k_y a_0}{2}\right)} \tag{6}$$
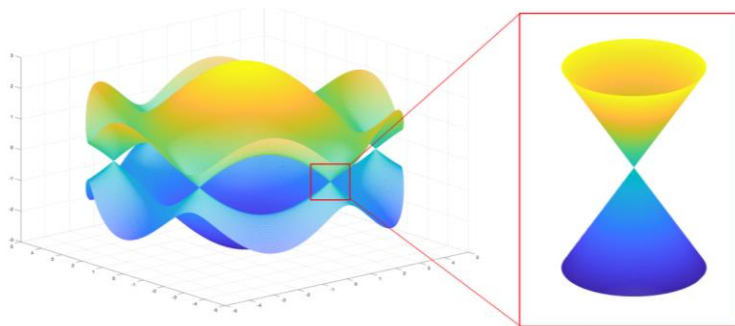

Figure 3. (Left) The electron band dispersion of monolayer graphene. (Right) Dirac cones in the corner of the Brillouin Zone of monolayer graphene

We can observe that monolayer graphene has a very special electron band structure:

1) The band surface of the two eigenvalues in the Brillouin Zone are almost mirror symmetric.

2) Two surfaces touch at the corner K points. At each corner the bands form two cones connected to each other on their ends at the Fermi level called "Dirac cones". The Dirac cones cause electrons in the monolayer to appear massless, meaning they can move at relativistic speeds. This makes graphene an extremely good conductor.

2.2 Atomic and Electronic Structure of Bilayer Graphene

In graphite, the stacking of graphene takes the AB, or Bernal, configuration. Graphene may also stack in the AA configuration. These two typical configurations are shown in Figure 4. In AA stacking, both layers are lined up; while in AB stacking, the layers are staggered. AB stacking is also analogous to twisting the layers of AA-stacked graphene 60° apart.
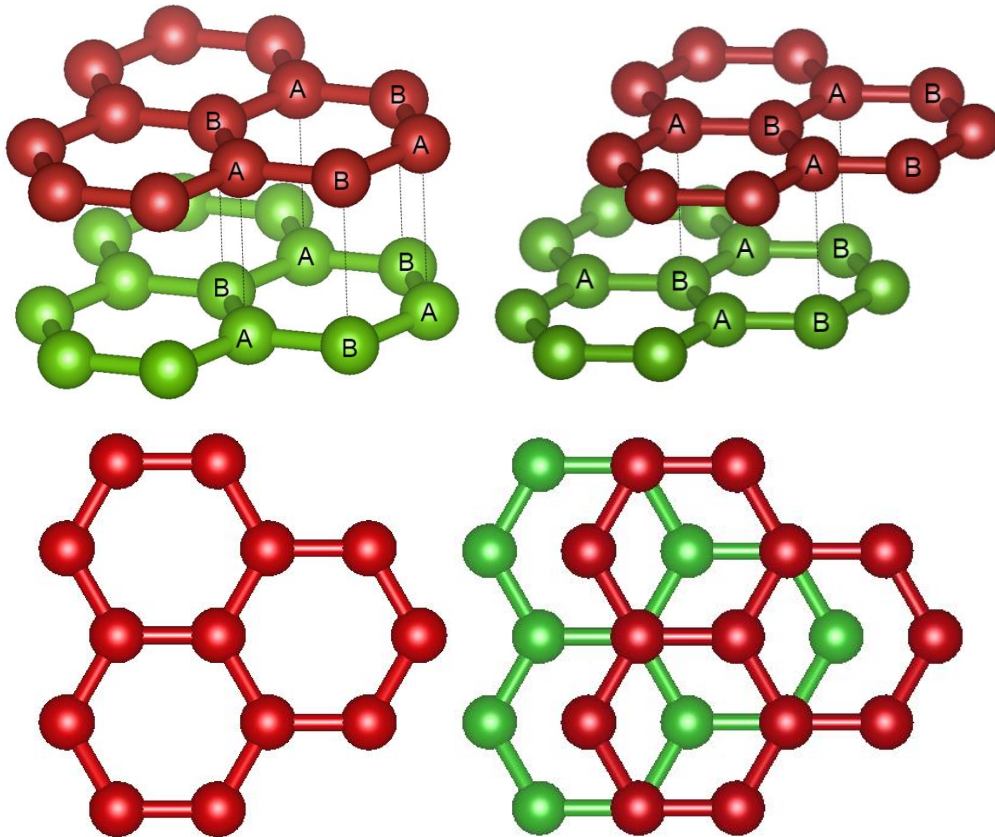

Figure 4. (Upper Left) AA stacking; atom "a" in top layer lines up with atom "a" in bottom layer, atom "b" in top layer lines up with atom "b" in bottom layer. (Upper Right) AB stacking; atom "a" in top layer lines up with atom "b" in bottom layer, atom "b" in top layer and atom "a" in bottom layer do not line up with anything. (Bottom) Top-down view of both AA and AB stacking configurations

Using a method similar to calculating the electronic band of monolayer graphene, we can construct the following matrixes for AA and AB configurations.

For AA configuration:

$$
\begin{array}{c|cccc}
 & A_u & B_u & A_d & B_d \\
\hline
A_u & \varepsilon_A - \varepsilon & E_1 f & E_2 & 0 \\
B_u & E_1 f^* & \varepsilon_B - \varepsilon & 0 & E_2 \\
A_d & E_2 & 0 & \varepsilon_A - \varepsilon & E_1 f \\
B_d & 0 & E_2 & E_1 f^* & \varepsilon_B - \varepsilon
\end{array} = 0 \qquad (7)
$$

And for AB configuration:

$$
\begin{array}{c|cccc}
 & A_u & B_u & A_d & B_d \\
\hline
A_u & \varepsilon_A - \varepsilon & E_1 f & 0 & E_2 \\
B_u & E_1 f^* & \varepsilon_B - \varepsilon & 0 & 0 \\
A_d & 0 & 0 & \varepsilon_A - \varepsilon & E_1 f \\
B_d & E_2 & 0 & E_1 f^* & \varepsilon_B - \varepsilon
\end{array} = 0 \qquad (8)
$$

Both of them give rise to very different band dispersions and band structures, as indicated in the right panels of Figure 5. Diagonalizing the above matrixes, we have

$$\varepsilon = \pm \ (E_2 \pm \tfrac{3}{2} ka E_1) \text{ for AA}; \quad \varepsilon_1 = \pm E_2 [1 + (\tfrac{3}{2} a \tfrac{E_1}{E_2})^2 \, q^2] \text{ and } \ \varepsilon_2 = \pm E_2 [0 + (\tfrac{3}{2} a \tfrac{E_1}{E_2})^2 \, q^2] \text{ for AB}$$
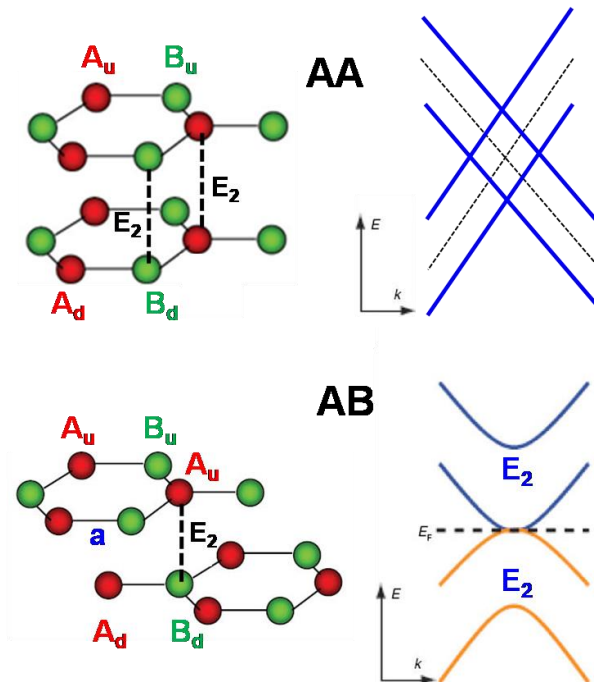

Figure 5. Interlayer hopping term and electronic band in AA (Top) and AB (Bottom) configurations

In the bilayer graphene with AA stacking configuration, the electron bands of both layers are aligned, so the AA-stacked bilayer has similar properties to a monolayer. In AB stacked bilayer graphene, the interlayer vdW force significantly reduce its carrier mobility. The two layers' electron bands also interfere with each other, leading to a decrease in the conductivity of AB stacked bilayer graphene. We notice here that stacking two layers changes the electronic band structure of graphene greatly. Again, as mentioned earlier, AB stacking can be considered to be twisted bilayer graphene from AA stacking by 60°. It is curious whether band structure changes continuously with the twist angle.

3. Atomic Structure and Electronic Band of Twisted Bilayer Graphene

Graphene has three-fold rotational symmetry, that is to say, the periodic rotating angle is 120°. In the meantime, there exists vertical mirror symmetry, suggesting that 60° is the smallest angle unit. 0° and 60° twist angle represent the AA and AB stacking, respectively. However, unlike the simple AA and AB stackings, the unit cell size for a twist angle between 0° and 60° becomes more complicated, depending on the twist angle (Moon & Koshino, 2013; Koshino, 2015). Figure 6 shows three twist angles at 21.7°, 31.3°, and 7.4° from left to right.

Moiré patterns can be created when the twist angle between two graphene layers are small. A moiré pattern is an interference pattern created when two layers of patterns are overlaid with each other. Twisted bilayer graphene (TBG) creates different moiré patterns depending on the amount of twist between layers.
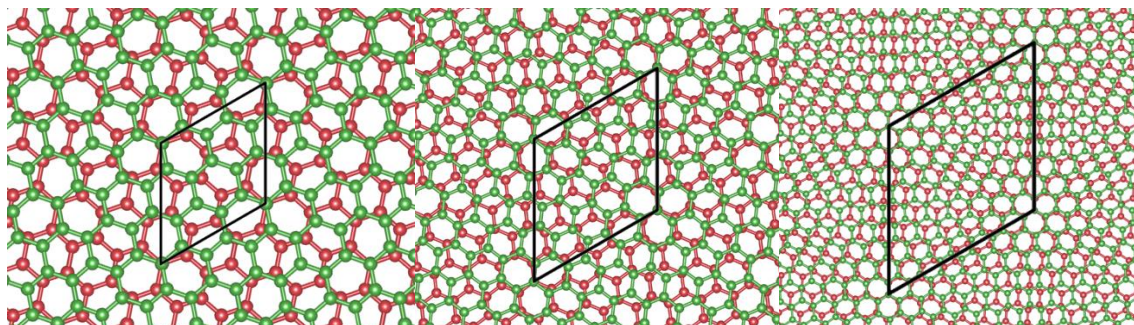

Figure 6. Moiré patterns at different turning angles (21.7, 13.3, and 7.44 from left to right) and their unit cells. These angles are just used as examples and do not have any significance to the rest of the paper

Figure 7 shows an analysis on the lattice parameters of TBG moiré lattice starting from the AA configuration. We first select a lattice vector $\mathbf{L}_b = m \ \vec{a}_1 + n\vec{a}_2$ in the bottom layer and $\mathbf{L}_t = n\vec{a}_1 + m \ \vec{a}_2$ in the top layer ($|L_b| = |L_t|$). We then rotate L_t to L_b by angle θ to form a TBG moiré lattice. We see that the lattice size L (L = $|L_b| = |L_t|$) for the TBG moiré lattice is

$$L = a\sqrt{m^2 + n^2 + mn} = \frac{|m-n|}{2\sin(\frac{\theta}{2})} a \qquad (9)$$

And the twist angle θ is

$$\cos(\theta) = \frac{1}{2} \frac{m^2 + n^2 + 4mn}{m^2 + n^2 + mn} \qquad (10)$$

As indicated by the black arrows in the right panel of Figure 7, both δL_1^M and δL_2^M should have the same and the smallest length —a, the graphene unit vector size — and take the vectors of ($\mathbf{a}_2$ - $\mathbf{a}_1$) and (–$\mathbf{a}_1$), respectively. The relation between the moiré lattice vectors $\mathbf{L}_1^M$ and $\mathbf{L}_2^M$ and the change ($\delta \mathbf{L}_1^M$ and $\delta \mathbf{L}_2^M$) to the moiré lattice vectors is

$$\boldsymbol{L}_1^M = \frac{(-\boldsymbol{a}_1 + \boldsymbol{a}_2) \times \boldsymbol{e}_z}{2\sin(\frac{\theta}{2})} \quad , \qquad \boldsymbol{L}_2^M = \frac{-\boldsymbol{a}_1 \times \boldsymbol{e}_z}{2\sin(\frac{\theta}{2})} \qquad (11)$$
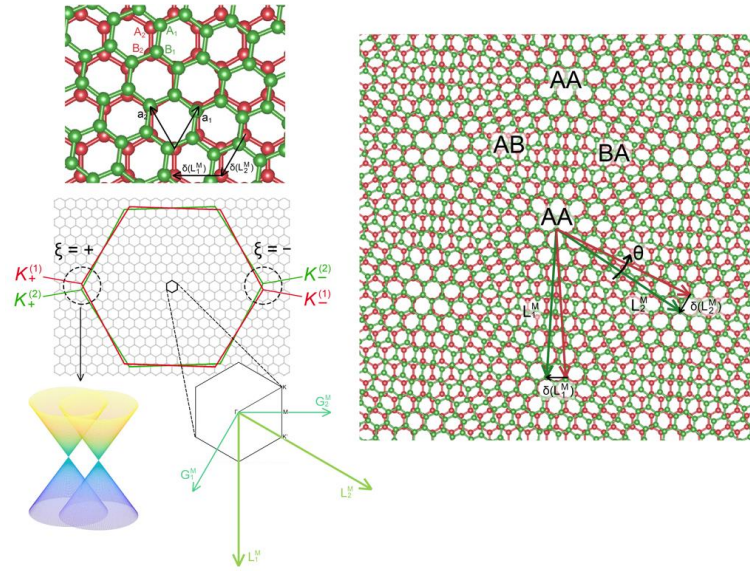
Figure 7. Lattice and reciprocal parameters of moiré patterns

4. The Effective Continuum Model and Electronic Band of TBG

With the information of unit cell parameters of moiré lattice, we can further analyze the corresponding lattice in the reciprocal space. As shown in the left lower corner of Figure 7, a twist in real lattice will induce a twist with the same angle in the reciprocal lattice. The Dirac cones of both layers form new hexagonal corners (K points) and new saddle points (M points) between. The reciprocal lattice vectors are

$$G_1^M = \frac{2\pi(L_2^M \times L_3^M)}{L_1^M \cdot (L_2^M \times L_3^M)} \quad G_2^M = \frac{2\pi(L_3^M \times L_1^M)}{L_1^M \cdot (L_2^M \times L_3^M)} \tag{12}$$

The tight-binding model of the TBG for p_z atomic orbital can be written as,

$$H = -\sum_{i,j} t(\boldsymbol{R}_i - \boldsymbol{R}_j)|\boldsymbol{R}_i\rangle\langle\boldsymbol{R}_j| \tag{13}$$

where $\boldsymbol{R}_i$ and $|\boldsymbol{R}_i\rangle$ represent the ith lattice point and the ith atomic states, respectively. And $t(\boldsymbol{R}_i - \boldsymbol{R}_j)$ refers to the hopping integral between the ith and j^{th} site. An approximation is adopted as follows,

$$-t(\boldsymbol{d}) = V_{pp\pi}\left[1 - \left(\frac{\boldsymbol{d}\cdot\boldsymbol{e_z}}{d}\right)^2\right] + V_{pp\sigma}\left(\frac{\boldsymbol{d}\cdot\boldsymbol{e_z}}{d}\right)^2 \tag{14}$$

$$V_{pp\pi} = V_{pp\pi}^0 exp\left(-\frac{d-a_0}{\delta_0}\right) \tag{15}$$

$$V_{pp\sigma} = V_{pp\sigma}^0 \exp\left(-\frac{d-d_0}{\delta_0}\right) \tag{16}$$

where a_0 is the atomic distance between the nearest A and B sites in graphene, and $d_0 = 0.335\ nm$ is the interlayer spacing. $V_{pp\pi}^0$ is the hopping integral between two π orbitals of the closest atoms of graphene and $V_{pp\sigma}^0$ is between the π orbitals of two vertically closest atoms between the neighboring sublayers. In this case, we use $V_{pp\pi}^0 = -2.7\ eV$ and $V_{pp\sigma}^0 = 0.48\ eV$ which can well fit the dispersive electronic bands of both monolayer and AB-stacked bilayer graphene. δ_0 is the decaying length of both the intralayer and interlayer hopping integral.

At a small rotation angle, the superlattice period of Moiré pattern is much bigger than the lattice size of monolayer graphene, only the long-wavelength components of the interlayer interaction remains. So, the twist bilayer graphene system can be treated by the effective continuum model. The continuum model can be constructed from tight-binding model. The Bloch basis of this system are

$$|\boldsymbol{k}, X_l\rangle = \frac{1}{\sqrt{N}}\sum_{\boldsymbol{R}_{X_l}} e^{i\boldsymbol{k}\cdot\boldsymbol{R}_{X_l}}|\boldsymbol{R}_{X_l}\rangle \tag{17}$$

where l is the layer index and N is the repetition of the monolayer unit cells in the TBG. And X=A, B is the sublattice of the monolayer graphene. k is the wave vector defined in the Moiré Brillouin zone (MBZ).

The continuum model of TBG can be written in the Bloch basis. The intralayer matrix element can be written as

$$h(\boldsymbol{k}, \boldsymbol{\tau}) = \sum_{n1,n2} -t(n_1\boldsymbol{a}_1 + n_2\boldsymbol{a}_2 + \boldsymbol{\tau}) \times \exp[-i\boldsymbol{k} \cdot (n_1\boldsymbol{a}_1 + n_2\boldsymbol{a}_2 + \boldsymbol{\tau})] \tag{18}$$

where $\boldsymbol{\tau}$ is the vector linking site B with site A. The spectrum of the monolayer graphene at low-energy scale is taken care of approximately by the Dirac cones around **K** and **K'** point. In the unrotated graphene we take **K** = $(2\pi/a)(-2/3, 0)$ and **K'** = $(2\pi/a)(2/3, 0)$. The **K** points of layer l in the rotated graphene are given by $\boldsymbol{K}^{(l)} = R(\mp\theta/2)\boldsymbol{K}$ and $\boldsymbol{K}'^{(l)} = R(\mp\theta/2)\boldsymbol{K}'$ in which $\mp$ represents for l = 1 and 2, respectively. The intralayer (within the layer) coupling continuum model in the vicinity of the K and K' is

$$H_l = -\hbar v[R(\mp\theta/2)(\boldsymbol{k} - \boldsymbol{K}_\xi^{(l)})] \cdot (\xi\sigma_x, \sigma_y) \tag{19}$$

where $\xi = \pm$ is the valley index and v is the fermi velocity of monolayer graphene. The σ_x and σ_y is the Pauli matrix and θ is the relative twist angle between graphene layers.

For the interlayer coupling, the matrix element in the Bloch basis is

$$U_{X_2 X_1} = -\frac{1}{\sqrt{N_1 N_2}}\sum_{R_{X_1} R_{X_2}} -t(\boldsymbol{R}_{X_2} - \boldsymbol{R}_{X_1})e^{i\boldsymbol{k}\cdot\boldsymbol{R}_{X_1} - i\boldsymbol{k}\prime\cdot\boldsymbol{R}_{X_2}} \tag{20}$$

where $\boldsymbol{R}_{X_1}$ and $\boldsymbol{R}_{X_2}$ are the atomic site in the layer 1 and 2. The N_1 and N_2 are the number of the monolayer unit cells. The interlayer coupling matrix can be Fourier transformed as

$$U_{X_2 X_1} = -\sum_{G,G'} \tilde{t}(\boldsymbol{k} + \boldsymbol{G})e^{-i\boldsymbol{G}\cdot\boldsymbol{\tau}_{X_1} + i\boldsymbol{G}\prime\cdot\boldsymbol{\tau}_{X_2}} \tag{21}$$

where $\tilde{t}(\boldsymbol{k} + \boldsymbol{G})$ is the in-plane Fourier transformation of the hopping integral $t(\boldsymbol{R}_{X_2} - \boldsymbol{R}_{X_1})$ defined by

$$\tilde{t}(\boldsymbol{k} + \boldsymbol{G}) = \frac{1}{S}\int t(\boldsymbol{R}_{X_2} - \boldsymbol{R}_{X_1})e^{-i(k+G)\cdot\boldsymbol{R}}d\boldsymbol{R} \tag{22}$$

with S is the area of the monolayer graphene and **R** is in-plane distance between two atomic sites whose integral is taken over an infinite two-dimensional space. We only consider the electronic states near $\boldsymbol{K}_\xi$ point, and the interlayer coupling matrix can be approximated as

$$U = \begin{pmatrix} U_{A_2 A_1} & U_{A_2 B_1} \\ U_{B_2 A_1} & U_{B_2 B_1} \end{pmatrix} = \tilde{t}(\boldsymbol{K})\left[\begin{pmatrix} 1 & 1 \\ 1 & 1 \end{pmatrix} + \begin{pmatrix} 1 & \omega^{-\xi} \\ \omega^\xi & 1 \end{pmatrix}e^{i\xi G_1^M \cdot r} + \begin{pmatrix} 1 & \omega^\xi \\ \omega^{-\xi} & 1 \end{pmatrix}e^{i\xi(G_1^M + G_2^M)\cdot r}\right] \tag{23}$$

where we have $\omega = \exp(i2\pi/3)$ and $\tilde{t}(\boldsymbol{K}) = 0.103 eV$ in the present tight-binding parameters.

The electronic structure of twisted bilayer graphene can be approximated using the following two equations (Koshino, 2015):

$$H_l = -\hbar v[R(\mp\theta/2)(\boldsymbol{k} - \boldsymbol{K}_\xi^{(l)})] \cdot (\xi\sigma_x, \sigma_y) \tag{24}$$

For interlayer interactions, where $\xi = \pm$ is the valley index, v is the fermi velocity of monolayer graphene, σ_x and σ_y are the Pauli matrices, and θ is the relative twist angle between graphene layers; and

$$U = \begin{pmatrix} U_{A_2 A_1} & U_{A_2 B_1} \\ U_{B_2 A_1} & U_{B_2 B_1} \end{pmatrix} = \tilde{t}(\boldsymbol{K})\left[\begin{pmatrix} 1 & 1 \\ 1 & 1 \end{pmatrix} + \begin{pmatrix} 1 & \omega^{-\xi} \\ \omega^\xi & 1 \end{pmatrix}e^{i\xi G_1^M \cdot r} + \begin{pmatrix} 1 & \omega^\xi \\ \omega^{-\xi} & 1 \end{pmatrix}e^{i\xi(G_1^M + G_2^M)\cdot r}\right] \tag{25}$$

For intralayer interactions, where $\omega = \exp(i2\pi/3)$ and $\tilde{t}(\boldsymbol{K}) = 0.103 eV$.

Combining these, we get the Hamiltonian of TBG:

$$H = \begin{pmatrix} H_1 & U^\dagger \\ U & H_2 \end{pmatrix} \tag{26}$$

We used a MATLAB program to draw the electron band structure of TBG by dividing the reciprocal unit cell into many points and calculating the Hamiltonian for each of those points. We can also find the density of states (DOS) — a measure that describes the number of electron states per unit volume per unit energy of a system — by

counting how many points on the electron band structure are on each energy level, but since we cannot calculate all the points on the electron band structure, we use this equation to approximate the DOS:

$$g(E) = \int_{BZ} \frac{d^2\boldsymbol{k}}{4\pi^2} \delta(E - E(\boldsymbol{k})) \tag{27}$$

Figure 8 shows the electronic band structure and the DOS of TBG at twist angles of 0.8°, 1.1°, 1.4°, 1.7°, and 2.0°.
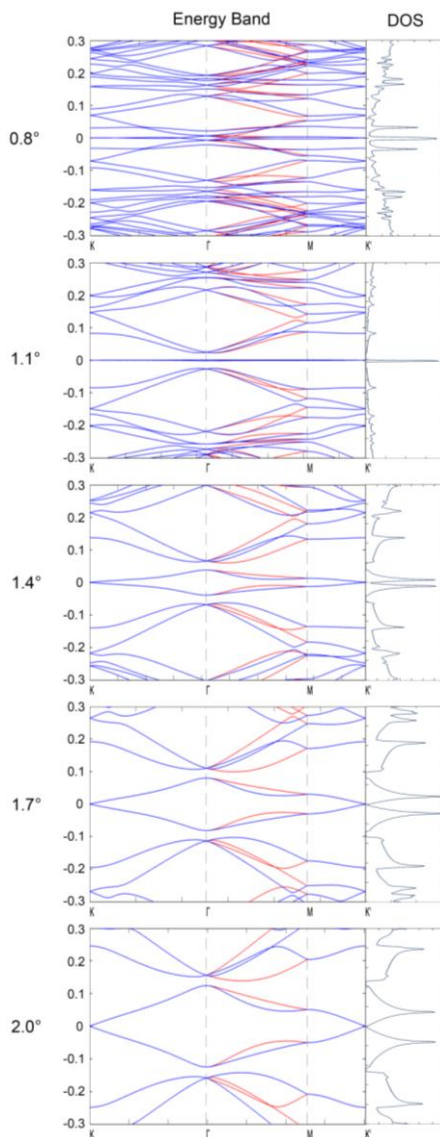

Figure 8. Electronic band and DOS of TBG at twist angles of 0.8°, 1.1°, 1.4°, 1.7°, and 2.0°

5. Magic Angle Twisted Bilayer Graphene

We realize that the band width and the distance between two diverging DOS van Hove singularities at the Fermi level decrease as the twist angle decreases from 2.0°. At turning angles close to magic angles (such as 1.1° in Fig 7), there is a very large spike right in the middle of the DOS. This spike indicates a flat band, which is when the electron bands are nearly completely flat. We can also detect flat bands by looking at the band width of the electron band structure, since flat bands have very small band widths due to being flat. We can see the relationship between twist angle and band width by calculating the band width as progressively increasing angles using the MATLAB program (Figure 9). We can see that there are more than one "magic angle" where flat bands appear. 0.4°, 0.9°, and 1.1° are close approximations of the 1st, 2nd, and 3rd magic angles.
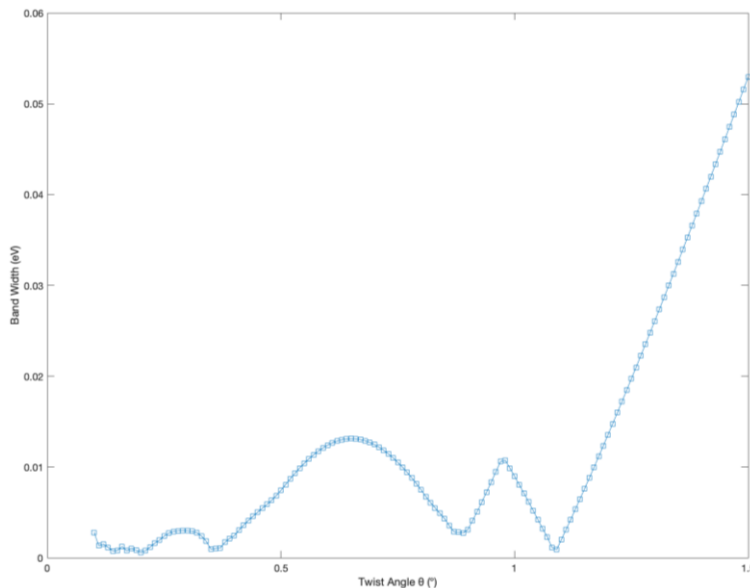
Figure 9. Width of flat band as a function of twist angle

TBG at these "magic angles" are dubbed magic angle twisted bilayer graphene, or MATBG. The most important of these special properties is the creation of "flat bands", where sections of the electron band structure are nearly completely flat.
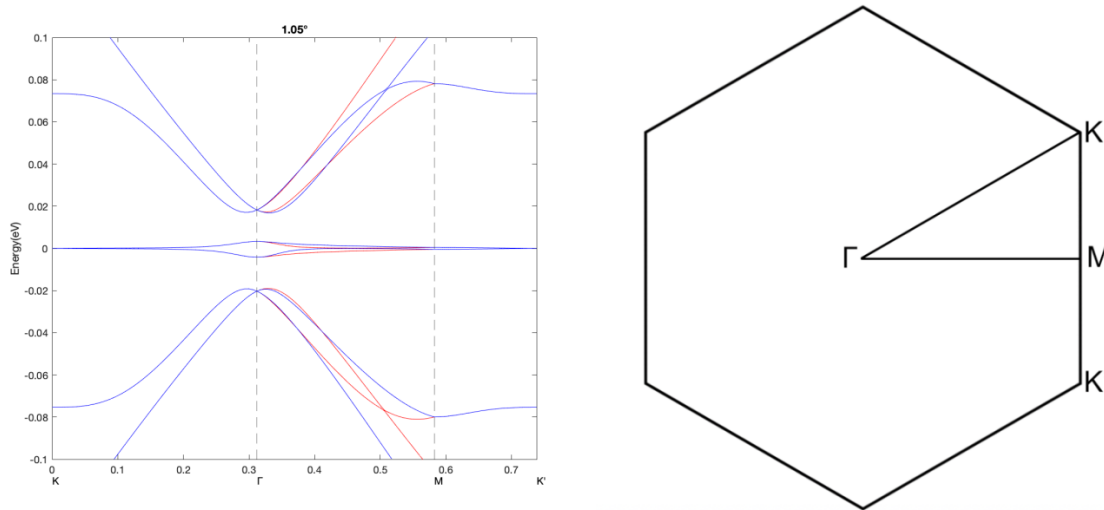

Figure 10. Electron band structure of 1.05° TBG from along points K, Γ, M, K'. The two inner most bands are very flat

The flat bands cause electrons in a material to appear to have nearly infinite mass or zero velocity. It becomes more easily for the slow electrons to see each other and to feel the Coulomb repulsion between each other, which is the so-called strong correlation phenomenon and most probably leads the material to become superconductive upon doping, just like what happens in the high-T_c superconductors.

6. Discussion

Monolayer graphene also has flat bands, though not enough to give it superconductive properties. These flat bands are around saddle points in the monolayer's electron band structure, where there are some relatively leveled zones.

In TBG, the twist creates some new saddle points when the Dirac cones of the two layers' electron bands intersect. At magic angles, very flat bands are created.

The emergence of flat bands with twist is still not clear in physics. Allen MacDonald and his colleagues from UT Austin considered that the electrons at the magic angle will quantum-tunnel with much higher probability between the top and bottom layers, leading to a slow-down within each layer. We speculate that the flat band may be understood more simply from the evolution of band structure from bilayer AA to AB stacking graphene. Looking back to Figure 5, band dispersion changes from linear in AA to quadratic in AB, suggesting that AB can suppress the electronic relativistic motion observed in monolayer graphene. The AB local stacking structure coexisting with the AA stacking in one twisted moiré superlattice can therefore contribute to the slow-down of electron. Reducing the twist angle increases the unit cell size of moiré superlattice and the size of the AB stacking structure, until magic angles are reached, where a total suppression of in-plane motion is gained, and a flat band appears.

7. Conclusion

Combining the tight-binding with the effective continuum models, we studied the electronic structures of monolayer, bilayer and twisted bilayer graphene, and demonstrated that "more is different" exists in the nanoscale from a single atomic layer to a double layer. In the double layer twisted moiré superlattice, we detected new and unique features of high-T_c superconductors, for example, flat band the related physical properties, which are not found in a single layer. This may arise from the symmetry breaking at quantum scale.

Conflict of interests

The authors declare that there is no conflict of interests regarding the publication of this paper.

References

Anderson, P. W. (1972). More is different. *Science, 177*(4047), 393-396. https://doi.org/10.1126/science.177.4047.393

Bistritzer, R., & MacDonald, A. H. (2011). Moiré bands in twisted double-layer graphene. *PNAS, 108*, 12233. https://doi.org/10.1073/pnas.1108174108

Cao, Y., Fatemi, V., Demir, A., Fang, S., Tomarken, S. L., Luo, J. Y., Sanchez-Yamagishi, J. D., Watanabe, K., Taniguchi, T., Kaxiras, E., Ashoori, R. C., & Jarillo-Herrero, P. (2018). *Nature(London), 556*, 80. https://doi.org/10.1038/nature26154

Cao, Y., Fatemi, V., Fang, S., Watanabe, K., Taniguchi, T., Kaxiras, E., & Jarillo-Herrero, P. (2018). Unconventional Superconductivity in Magic-Angle Graphene Superlattices. *Nature(London). 556*, 43. https://doi.org/10.1038/nature26160

Koshino, M. (2015). Interlayer interaction in general incommensurate atomic layers. *New J. Phys., 17*, 015014. https://doi.org/10.1088/1367-2630/17/1/015014

Moon, P., & Koshino, M. (2013). Optical absorption in twisted bilayer graphene. *Physical Review, B87*, 205404. https://doi.org/10.1103/PhysRevB.87.205404

Novoselov, K. S., Geim, A. K., Morozov, S. V., Jiang, D., & Katsnelson, M. I. (2005). Two-dimensional gas of massless Dirac fermions in graphene. *Nature, 438*(7065), 197-200. https://doi.org/10.1038/nature04233

Novoselov, K. S., Geim, A. K., Morozov, S. V., Jiang, D., Zhang, Y., Dubonos, S. V., Grigorieva, I. V., & Firsov, A. A. (2004). Electric field effect in atomically thin carbon films. *Science, 306*(5696), 666-669. https://doi.org/10.1126/science.1102896

Wallace, P. R. (1947). The Band Theory of Graphite. *Physical Review, 71*, 622-634. https://doi.org/10.1103/PhysRev.71.622

Copyrights